Earth Planets Space, **58**, 1165–1171, 2006

Dynamics and Energetics of the Lower Thermosphere in Aurora (DELTA) —Japanese sounding rocket campaign—

Takumi Abe[1], Junichi Kurihara[1], Naomoto Iwagami[2], Satonori Nozawa[3], Yasunobu Ogawa[3], Ryoichi Fujii[3], Hajime Hayakawa[1], and Koh-ichiro Oyama[1]

[1]*Institute of Space and Astronautical Science, Japan Aerospace Exploration Agency, 3-1-1, Yoshinodai, Sagamihara, Kanagawa 229-8510, Japan*
[2]*The University of Tokyo, Bunkyo-ku, Tokyo 113-0033, Japan*
[3]*Solar-Terrestrial Environment Laboratory, Nagoya University, Nagoya, Aichi, 464-8601, Japan*

(Received November 25, 2005; Revised July 8, 2006; Accepted July 26, 2006; Online published September 29, 2006)

Japanese sounding rocket "S-310-35" was launched from Andøya Rocket Range in Norway on December 13, 2004 during Dynamics and Energetics of the Lower Thermosphere in Aurora (DELTA) campaign, in which the rocket-borne in-situ measurements and ground-based measurements were coordinated to carry out a comprehensive observation of the thermospheric response against the auroral energy input. The instruments on board the rocket successfully performed their measurements during the flight, and thereby the temperature and density of molecular nitrogen, auroral emission rate, and the ambient plasma parameters were derived. Simultaneous measurements by the ground-based instruments provided neutral wind, neutral temperature, the auroral images and the ionospheric parameters near the rocket trajectory. This paper introduces science objectives, experimental outline, and preliminary scientific results of the DELTA campaign and explains geophysical condition at the time of the rocket launch, while the companion papers in this special issue describe more detailed results from each instrument.

Key words: Lower thermosphere, dynamics, energetics, sounding rocket, aurora.

1. Science Background

Auroral energy inputs from the magnetosphere in the form of electric fields and energetic particles are deposited mainly in the lower thermosphere (90–150 km) by Joule and particle heating, and the dissipation rates of the auroral energies can exceed that of other energy sources such as solar ultraviolet radiation (Roble, 1995; Thayer and Semeter, 2004). Ion drag, which is the force exerted on neutral species by ions accelerated by the electric fields through ion-neutral collisions, transfers momentum to the neutral atmosphere and drives the neutral winds (Larsen *et al*., 1995; Richmond and Thayer, 2000). Moreover, collisions of precipitating particles with the neutral species lead to an increase in ionospheric conductivity, various chemical processes of ions and neutral species, changes in composition, and auroral emissions (Rees, 1989; Schunk and Nagy, 2000). For a better understanding of the complex interactions between the dynamics and the energetics in the coupled magnetosphere-ionosphere-thermosphere system, it is important to investigate the atmospheric response to auroral activities.

Recent observations in the polar thermosphere have revealed the strong atmospheric response to auroral energy inputs. Strong neutral winds and wind shears are observed in the polar lower thermosphere during auroral disturbances using the chemical release technique in the series of Atmospheric Response in Aurora (ARIA) rocket experiments (Larsen *et al*., 1997). The observed wind profiles show the presence of a jet around 110–120 km altitudes. The wind speeds of the jets increase and the hodograph is more likely linear as the geomagnetic activity level increases. Richardson numbers in the shear regions below the jets are calculated based on the atmospheric model and are close to or below the critical value of 0.25, suggesting that flow is highly unstable. In such an unstable shear, turbulence will be generated and enhancement of the eddy diffusivity can lead to compositional changes. Parish *et al*. (2003) performed simulations using a three-dimensional high-resolution model and parameters measured in the ARIA campaign, and showed that large winds are generated by auroral forcing. The vertical structures of winds are simulated well when propagating tides are included in the background winds although the magnitude of the jet is much smaller than that observed. Their results suggest that a combination of auroral and tidal forcing controls the magnitude of the jet and that a combination of different tidal modes contributes the vertical structure. Fujiwara *et al*. (2004) estimated turbulent energy dissipation rates and electromagnetic energy dissipation rates in the polar lower thermosphere using neutral wind, ionospheric conductivity, and electric field data obtained from the European Incoherent Scatter (EISCAT) Svalbard radar observations. The derived neutral wind fields show strong vertical shears and temporal variations. They found that the turbulent energy dissipation rate is dominant below 109 km on average while an electromagnetic energy dissipation rate is domi-

nant above the altitude. The two energy dissipation rates, which are affected by the neutral wind, can be the main heat sources in the polar lower thermosphere. These results indicate that the neutral wind field is influenced not only by the ionosphere-thermosphere coupling but also by the lower atmospheric process. Thus, there exist various theories and simulations to account for the causal relationship between the energy dissipation and the wind field. However, there have been no unified interpretations which can explain how and to what extent these two processes drives the neutral wind depending on the altitude in the polar lower thermosphere.

There have been a number of studies on vertical winds in the polar thermosphere (Rees *et al*., 1984; Crickmore *et al*., 1991; Price and Jacka, 1991; Conde and Dyson, 1995; Aruliah and Rees, 1995; Smith and Hernandez, 1995; Price *et al*., 1995; Innis *et al*., 1996, 1997, 1999; Ishii *et al*., 1999; Kosch *et al*., 2000; Ishii *et al*., 2001; Innis and Conde, 2002; Ishii *et al*., 2004). Rees *et al*. (1984) reported the Fabry-Perot Interferometer (FPI) observations of large vertical winds exceeding 50–200 m/s at the upper thermosphere associated with auroral disturbances. Price *et al*. (1995) first showed large upwelling occurring simultaneously in both the lower thermosphere and upper thermosphere and described the upwelling event near auroral arc using a schematic model. Recent observations suggest that vertical winds may be driven by localized heating such as particle and Joule heating (Price *et al*., 1995; Innis *et al*., 1999), by effect of positive or negative divergence of horizontal winds (Smith and Hernandez, 1995; Ishii *et al*., 2001), and by atmospheric gravity waves propagating from auroral oval (Johnson *et al*., 1995; Innis and Conde, 2002). Modeling studies suggest that large vertical winds have a significant impact on the dynamics and composition in the polar thermosphere (Walterscheid *et al*., 1985; Walterscheid and Lyons, 1992; Sun *et al*., 1995; Shinagawa *et al*., 2003).

In previous studies on the dynamics and energetics in the polar lower thermosphere, the main interest has been in neutral wind measurements. However, in order to discuss whether the atmosphere becomes actually unstable in the wind shear, calculations of Richardson number require not only the wind shear but also local temperature gradient measurements. In addition, the cause of vertical wind structures is not fully identified mainly because of uncertainty in the parameters necessary for modeling studies. One of the key parameters to be measured is neutral atmospheric temperature, which is also important for understanding thermal structure and energy budget for auroral heating process. The thermal structure depends on the heat sources such as turbulent and electromagnetic energy dissipations in the polar lower thermosphere. The existing empirical atmospheric models are uncertain because of the poor basis for the temperature measurement in this altitude range especially during auroral disturbances. Ground-based FPI is one of very limited tools for simultaneous measurements of neutral temperature and wind using auroral 557.7 nm emission in the lower thermosphere. Since the effective emission altitude of auroral 557.7 nm emission varies depending on the precipitating electron energy and vertical temperature gradients in the lower thermosphere are generally steep, there are difficulties in quantitative analysis of the neutral temperature derived only from the FPI observations.

To promote a better understanding of the above subject, Dynamics and Energetics of the Lower Thermosphere in Aurora (DELTA) campaign was planned, in which the sounding rocket, EISCAT radar, FPIs, sodium lidar, and other ground-based observations were coordinated so that it can provide a comprehensive description of the atmospheric response to auroral disturbances. In this paper, we present an outline of this campaign and an experimental summary of the campaign. Detailed scientific results derived from each instrument are given in the companion papers in this special issue.

2. Campaign Objectives

A comprehensive objective of the present campaign is to study the lower thermospheric dynamics and energetics caused by auroral energy input. Among various phenomena existing in the polar lower thermosphere, characteristic feature of the neutral wind, such as vertical wind or wind shear, has been observed to exist by in-situ and remote measurements, as described in the previous section. One of the most important phenomena which should be investigated by the present campaign is a vertical shear of strong neutral wind. It should be elucidated through this campaign study how such thermospheric wind field is driven by the energy inputs due to auroral particle precipitating from the higher magnetosphere, other electromagnetic force, and tidal forcing from the lower atmosphere. As a primary experiment in this campaign, the Japanese sounding rocket "S-310-35" was launched from Andøya rocket range in Norway on December 13, 2004. The ionospheric condition can continuously be measured by the EISCAT UHF radar in Tromsø. Information on neutral wind and temperature in the vicinity of the rocket trajectory is provided by FPIs in Skibotn and in KEOPS (Kiruna ESRANGE Optical Platform System) and sodium lidar in ALOMAR (Arctic Lidar Observatory for Middle Atmospheric Research). For this campaign, ground-based monitoring of the auroral activity and its distribution is also important because these parameters are closely related to the atmospheric dynamics observed on the rocket. The neutral wind and its shear may be highly structured in space, and these are known to change according to the level of geomagnetic activity. It is, therefore, important to understand how the sounding rocket was located in terms of the spatial distribution and temporal history of the auroral activity.

A coordinated observation of thermospheric neutral and ionospheric plasma parameters by a sounding rocket, FPI, and EISCAT is possibly the first attempt in the world. In particular, a comparison of in-situ neutral temperature measurements on the rocket with the ground-based measurements is expected to bring new dataset for the study of the energy budget in the lower thermosphere, because it has been unavailable so far despite its importance. For example, it is well known that the ground-based FPI measurements have a problem with the assumption of the auroral emission layer heights, and it is difficult to find a region where the thermospheric wind is measured. A comparison between in-situ measurement of neutral temperature by the NTV on

Table 1. List of the rocket-borne instruments

Instrument	Measurement Item	Position	Main Organization	Reference
NTV	Temperature and Density of N_2	Daughter payload	ISAS/JAXA	Kurihara *et al*. (2006)
APD	Electron energy spectrum		ISAS/JAXA	Ogasawara *et al*. (2006)
HOS	Rocket attitude		Univ. of Tokyo	Iwagami *et al*. (2006)
CLP	Relative variation of N_e		ISAS/JAXA	Abe *et al*. (2006)
AGL	Auroral (557.7 nm) emission rate	Mother payload	Univ. of Tokyo	Iwagami *et al*. (2006)
FLP	Electron temperature and density		ISAS/JAXA	Abe *et al*. (2006)
NEI	Electron density		Tohoku Univ.	Wakabayashi and Ono (2006)
SFF	Rocket attitude		Univ. of Tokyo	Iwagami *et al*. (2006)

the rocket and remote measurements by the FPI from the ground will provide information useful for estimating the effective emission height. Thus, an integrated analysis of the in-situ measurement and the ground based observation enables us to study the thermospheric dynamics or energetics from further insight. Moreover, it is possible to estimate Joule and particle heating rate from the EISCAT radar observations and photometer measurements on the ground. A quantitative comparison of these heating rates with neutral temperatures from the NTV and/or the FPI measurements can make it possible to discuss the atmospheric heating rate by auroral energy input. In the strict sense, the sounding rocket trajectory was located approximately 100 km away east from the EISCAT radar in Tromsø. A spatial distance between these observational points may exert undesirable influence on the coordinated analysis when the small scale wind structure is investigated.

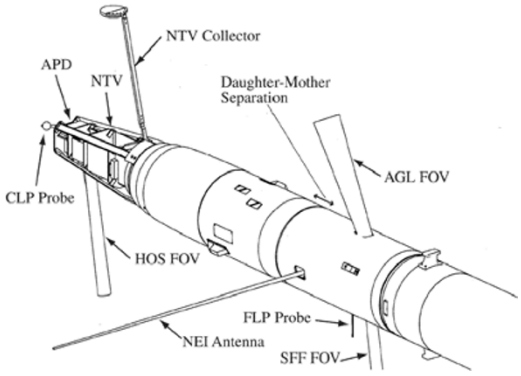

Fig. 1. Appearance of the sounding rocket for the DELTA campaign.

3. Instrumentation

The sounding rocket was equipped with a suite of eight instruments to derive N_2 temperature and density, the auroral emission rate, the electron density and temperature, the energy distribution of precipitating electrons and the rocket attitude. The instrument to measure the temperature and density of molecular nitrogen, called NTV (Kurihara *et al*., 2006), is based on the electron beam fluorescence technique, and emits an electron beam with an energy of 1 keV from the rocket. In such a situation, the rocket body is thought to be positively charged, which has an unfavorable influence on the passive measurements by the Langmuir probe and the impedance probe. To avoid this interference, the rocket was separated into two sections; mother payload (section close to the rocket motor) and daughter payload (upper section), at the altitude of 100 km during the rocket's ascending phase. The NTV was installed on the daughter payload section while the passive instruments being on the mother. Table 1 explains instruments installed on the mother and daughter payloads.

On the daughter-payload section, the NTV instrument measures rotational and vibrational temperatures and number density of molecular nitrogen (N_2) in the altitude range from 100 to 140 km. The CLP (Constant biased Langmuir Probe) is used to find a relative variation of electron density measured by a spherical probe biased with a positive voltage. The role of the APD (Auroral Particle Detector) is to provide electron energy spectrum and the pitch angle distribution in the energy range from 3 to 60 keV using avalanche photodiodes (Ogasawara *et al*., 2006). The HOS (Horizon Sensor) adopts an infrared sensor to detect the direction of the horizon from the rocket to determine the attitude of the daughter payload section (Iwagami *et al*., 2006).

As for the mother-payload instruments, the AGL (Auroral Green Line photometer) measures the column emission rate of the auroral green line (OI 557.7 nm) using a narrow band filter, and thereby the total energy input into the atmosphere and the characteristic energy of the precipitating particles can be estimated (Iwagami *et al*., 2006). In the FLP (Fast Langmuir Probe) instrument, a cylindrical probe with a length of 140 mm and a diameter of 3 mm is deployed in the direction perpendicular to the rocket's spin axis, and the electron temperature and density can be estimated by elucidating the probe V-I characteristics (Abe *et al*., 2006). The NEI (Impedance probe) instrument measures the Upper Hybrid Resonance (UHR) frequency of the ambient plasma, from which the electron number density can be accurately derived, by detecting an equivalent capacitance of a ribbon antenna (Wakabayashi and Ono, 2006). In the SFF (Surface Finder) instrument, an infrared sensor detects the direction of the Earth's surface on the rocket to obtain attitude information of the mother-payload section (Iwagami *et al*., 2006). The appropriate reference of each instrument is given in the right-most row of Table 1. Figure 1 is a schematic view of the payload section of the sounding rocket launched for the DELTA campaign. The eight instruments are installed on the payload zone of the rocket. The deployment systems such as the NTV electron beam collector, the FLP probe, and the NEI antenna are operated by a timer signal during the flight.

Table 2. List of the ground-based instruments

Instrument	Measurement Item	Location	Main Organization	Reference
EISCAT UHF radar	T_e, N_e, T_i and Ion drift	Tromsø	STEL/Nagoya Univ. NIPR	Nozawa *et al*. (2006)
FPI	Neutral wind and temperature	Skibotn KEOPS	Lancaster Univ. (UK) UCL (UK)	Griffin *et al*. (2006)
Sodium lidar	Neutral temperature and wind	ALOMAR	Colorado State Univ. (US)	Williams *et al*. (2006)
MF radar	Wind field and N_e profile	ALOMAR Tromsø	IAP (Germany) (∗)	
Meteor radar	Wind field	ALOMAR Tromsø	IAP (Germany) NIPR	
Photometer	427.8, 630.0, 670.5, 844.6 nm	Tromsø	STEL/Nagoya Univ.	
All-sky camera	Auroral images	Tromsø Skibotn KEOPS Kilpisjärvi Andøya	Univ. of Calgary (Canada) Lancaster Univ. (UK) UCL (UK) FMI (Finland) ARR (Norway)	 Griffin *et al*. (2006) Griffin *et al*. (2006)

(∗) University of Tromsø (Norway), University of Saskatchewan (Canada), and Nagoya University

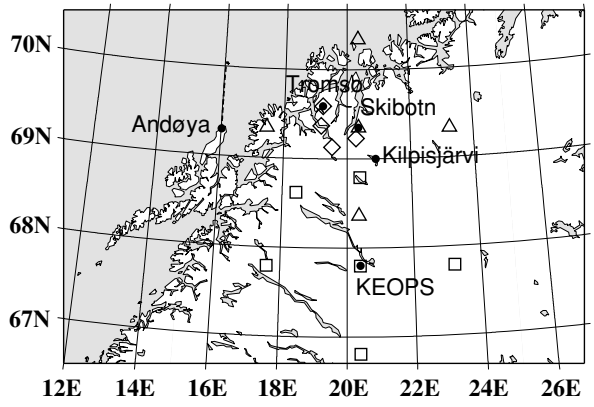

Fig. 2. Locations of Andøya rocket range, Tromsø UHF radar, the Skibotn FPI, KEOPS FPI, and all-sky camera in Kilpisjärvi (closed circles). A broken line represents the projection of the rocket trajectory. Open triangles, boxes, and diamonds denote the projections of the sampled volumes at 110 km for the Skibotn FPI (North, East, South, West, Zenith), KEOPS FPI (North, East, South, West, Zenith, Northwest), and EISCAT UHF radar beam positions (Vertical, field aligned, East1, East2), respectively.

A list of the coordinated ground-based instruments for the DELTA campaign is given in Table 2. During this campaign, the EISCAT UHF radar was mostly operated in the beam-scanning (CP2) mode, which provides the electron temperature and density, ion temperature and drift, and enables one to derive neutral wind velocity (Nozawa *et al*., 2006). It is important that the EISCAT radar can provide not only an instantaneous value but also a long-term trend of the above parameters, which is particularly important for the interpretation of the long-lived thermospheric phenomena such as the semidiurnal tide. Two FPIs in Skibotn and KEOPS detect the green line airglow and auroral emission at 557.7 nm (and also 630.0 nm at KEOPS) so that neutral winds and temperatures at the emission height can be estimated (Griffin *et al*., 2006). The line-of-sight winds and temperatures are estimated from the Doppler shift and broadening of the emission spectrum, respectively. In ALOMAR, a narrow-band sodium lidar system is operated to derive temperature and winds between 80 and 105 km, for investigating dynamics in the mesopause region (Williams *et al*., 2006). Combining the sodium lidar and in-situ rocket measurement, a continuous temperature profile over 80–140 km altitude range can be provided. Both in Andenes and in Tromsø, MF (Medium Frequency) radar system emits electromagnetic pulses which are vertically radiated by the transmit antenna and received by three spatial separated antennas after partial reflection on irregularities in the ionospheric D-region. Thus, MF radar can measure neutral wind and electron density profile in the upper mesosphere and lower thermosphere. In meteor radar system at ALOMAR, short electromagnetic pulses are radiated by the transmit antenna and after reflection on ionization trails of incident meteoroids received by five spatially separated antennas. An interferometric analysis yields location, amplitude and radial velocity of each ionization trail moved by the neutral wind. The wind field in the lower thermosphere can be derived from a multitude of individual information.

4. Rocket Launch and Geophysical Condition

The Japanese sounding rocket "S-310-35" was launched in the direction of geographical north at 00:33 UT of December 13, 2004, from Andøya Rocket Range in Norway. The rocket reached the maximum altitude of 140.0 km with a horizontal distance of 43.8 km at 184 sec from the launch. During its ascent, the rocket was separated into two parts; mother and daughter payloads, to avoid interference between the instruments. At 300 sec from the launch, the rocket passed through an altitude of 76.8 km with a horizontal distance of 72.6 km during its descent. Figure 2 shows the locations of the rocket range and the ground-based observation sites.

The EISCAT radar observations in Tromsø indicate that at 00:12 UT of December 13, the electron number density suddenly increased to more than 10^5 cm^{-3} in the ionospheric E region, probably due to ionization by the precipitating electrons along the magnetic field lines. Such a

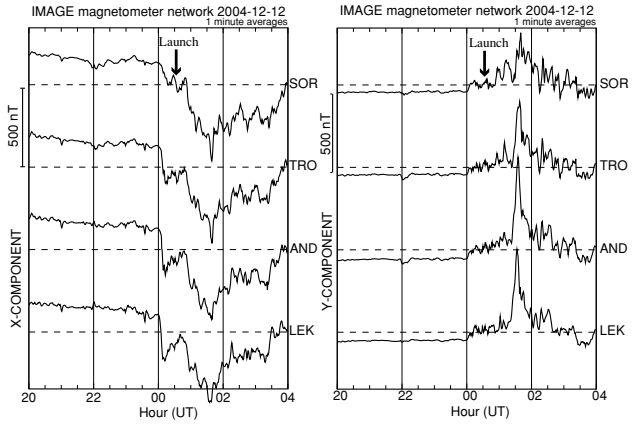

Fig. 3. Magnetogram data in four stations (Sørøya, Tromsø, Andenes, Leknes) from 20 UT on Dec. 12 to 04 UT on 13. Left: X-component (geographically northwards), Right: Y-component (geographically eastwards)

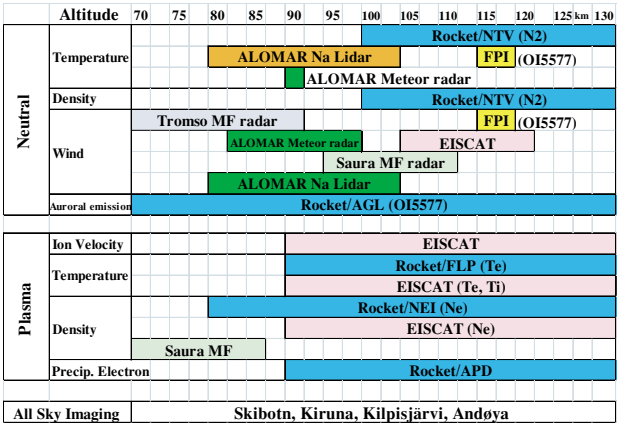

Fig. 4. Measurement item and altitude coverage of the rocket-borne and the ground-based instruments.

condition of the high electron density was continuously observed for more than one hour (see Nozawa *et al.*, 2006). This suggests that the precipitating electrons have successively given the energy input into the high-latitude lower thermosphere. Figure 3 shows the magnetogram data in four stations (Sørøya, Tromsø, Andenes, Leknes) from 20 UT on Dec. 12 to 04 UT on 13. The X and Y components of the magnetic field are defined as geographically northwards and eastwards, respectively. It is realized from the figures that the auroral jet current was predominantly flowing to the eastward for the time period from 0:00 UT to 3:30 UT over these four stations including Andenes where the rocket was launched.

At the time of the rocket launch, the sky was clear in KEOPS and mostly clear with thin cloud in Skibotn, and therefore two FPIs' observations were successfully operated (Griffin *et al.*, 2006). In contrast, it was completely cloudy in Tromsø and no useful data were obtained by the optical instruments such as photometer and all-sky imager. In Andøya, the sky had been clear until one hour before the launch but afterwards the visibility became poor due to clouds. The three-hourly Kp index was 4^+ for 00–03 UT on December 13. It should be noted that the B_z component of the IMF turned to negative at 22:07 UT on Dec. 12 (two and a half hours before the launch), which may be related to the electron density enhancement starting at 00:12 UT described above.

5. Observations

All the instruments on board the rocket successfully made in-situ measurements of neutral atmospheric temperature and density, auroral emission rate, electron density and temperature during the rocket's flight. The coordinated measurements by various optical and radar instruments on the ground also succeeded to get the data in and around the launch site. These observations provide information on the auroral activity and its spatial distribution, neutral wind, and atmospheric heating on a longer time scale.

The EISCAT UHF radar in Tromsø was continuously operated for 12 hours from 16 UT on December 12, with the CP2 mode. It provided the electron density, temperature, and ion velocity vector every 6 minutes in the E and F region as well as the electric field vector (Nozawa *et al.*, 2006). The FPIs in Skibotn and KEOPS continuously observed the line-of-site wind velocity and neutral temperature during the rocket campaign (Griffin *et al.*, 2006). Though it was cloudy at the time of launch, the Weber Na lidar at ALOMAR observatory was operating off and on between 20:00 UT and 23:30 UT on December 12, observing Na density, temperature and meridional wind between 80 and 100 km (Williams *et al.*, 2006). Figure 4 explains the altitude region for which the respective parameters were observed during the DELTA campaign. This indicates that various parameters inherent for understanding the dynamics and energetics in the lower thermosphere were successfully obtained, although no meaningful data were provided by some optical measurements in Tromsø. Detailed scientific results from the rocket-borne and the ground-based instruments are described in the companion papers in this special issue.

6. Scientific results

During the DELTA campaign, the rocket-borne in-situ measurements and ground-based measurements were coordinated to carry out a comprehensive observation of the lower thermospheric response against the auroral energy input. These are expected to bring a dataset substantial for a study of the dynamics and energetics in the lower thermosphere. Main results of the current analysis on the DELTA campaign data are summarized as follows:

1) The rotational temperature of molecular nitrogen (N_2) by the NTV at altitudes of 95–140 km is much higher than neutral temperature from the MSIS model. The FPI measurements at Skibotn and the KEOPS indicate that the neutral temperatures are close to the rotational temperature measured at 120 km altitude. (Kurihara *et al.*, 2006)
2) Energetic electron observations by the APD suggest that a spatial distribution of energetic electron precipitations is consistent with the all-sky camera images at 557.7 nm obtained in the surrounding ground-based

optical stations. (Ogasawara *et al.*, 2006)

3) The Langmuir probe measurements on the rocket identified a local increase of the electron temperature at an altitude of 107–115 km, The Farley-Buneman instability may be a possible candidate as a heating mechanism, because the small-scale electron density perturbations were detected in the probe current. (Abe *et al.*, 2006)
4) The EISCAT radar was successively operated with a beam-scanning mode at Tromsø during the DELTA campaign. Comparison of neutral temperatures measured by the NTV on the rocket and ion temperature by the EISCAT VHF radar show a reasonable agreement, while the electron temperatures from the rocket measurement and the EISCAT radar observation disagree with each other. (Nozawa *et al.*, 2006)
5) The auroral emission rate and electron density were significantly larger in the rocket's ascending than in the descending, which suggests that the rocket traversed a highly energized region in the first half of the flight. (Iwagami *et al.*, 2006; Wakabayashi and Ono, 2006)

Acknowledgments. We are deeply indebted to Prof. Thrane at Andøya Rocket Range for his extensive support for the DELTA campaign. This campaign was conducted as an international project that consists of many organizations and universities in Japan, Norway, UK, Finland, Germany, United States, and Canada. We thank all the staff of the rocket launch and the ground-based observations. We also thank the institutes who maintain the IMAGE magnetometer array, particularly Tromsø Geophysical Observatory, University of Tromsø. This work was carried out by the joint research program of the Solar-Terrestrial Environment Laboratory, Nagoya University.

References

Abe, T., K. I. Oyama, and A. Kadohata, Electron temperature variation associated with the auroral energy input during the DELTA campaign, *Earth Planets Space*, **58**, this issue, 1139–1146, 2006.

Aruliah, A. L. and D. Rees, The trouble with thermospheric vertical winds: geomagnetic, seasonal and solar cycle dependence at high latitudes, *J. Atmos. Terr. Phys.*, **57**, 597–609, 1995.

Conde, M. and P. L. Dyson, Thermospheric vertical winds above Mawson, Antarctica, *J. Atmos. Terr. Phys.*, **57**, 589–596, 1995.

Crickmore, R. I., J. R. Dudeney, and A. S. Rodger, Vertical thermospheric winds at the equatorward edge of the auroral oval, *J. Atmos. Terr. Phys.*, **53**, 485–492, 1991.

Fujiwara, H., S. Maeda, M. Suzuki, S. Nozawa, and H. Fukunishi, Estimates of electromagnetic and turbulent energy dissipation rates under the existence of strong wind shears in the polar lower thermosphere from the European Incoherent Scatter (EISCAT) Svalbard radar observations, *J. Geophys. Res.*, **109**, A07306, doi:10.1029/2003JA010046, 2004.

Griffin, E., M. Kosch, A. Aruliah, A. Kavanagh, I. McWhirter, A. Senior, E. Ford. C. Davis, T. Abe, J. Kurihara, K. Kauristie, and Y. Ogawa, Combined ground-based optical support for the aurora (DELTA) sounding rocket campaign, *Earth Planets Space*, **58**, this issue, 1113–1121, 2006.

Innis, J. L. and M. Conde, High-latitude thermospheric vertical wind activity from Dynamic Explorer 2 Wind and Temperature Spectrometer observations: indications of a source region for polar cap gravity waves, *J. Geophys. Res.*, **107**(A8), doi:10.1029/2001JA009130, 2002.

Innis, J. L., P. A. Greet, and P. L. Dyson, Fabry-Perot spectrometer observations of the auroral oval/polar cap boundary above Mawson, Antarctica, *J. Atmos. Terr. Phys.*, **58**, 1973–1988, 1996.

Innis, J. L., P. L. Dyson, and P. A. Greet, Further observations of the thermospheric vertical wind at the auroral oval/polar cap boundary above Mawson station, Antarctica, *J. Atmos. Terr. Phys.*, **59**, 2009–2022, 1997.

Innis, J. L., P. A. Greet, D. J. Murphy, M. G. Conde, and P. L. Dyson, A large vertical wind in the thermosphere at the auroral oval/polar cap boundary seen simultaneously from Mawson and Davis, Antarctica, *J. Atmos. Sol.-Terr. Phys.*, **61**, 1,047–1,058, 1999.

Ishii, M., S. Oyama, S. Nozawa, R. Fujii, E. Sagawa, S. Watari, and H. Shinagawa, Dynamics of neutral wind in the polar region observed with two Fabry-Perot interferometers, *Earth Planets Space*, **51**, 833–844, 1999.

Ishii, M., M. Conde, R. W. Smith, M. Krynicki, E. Sagawa, and S. Watari, Vertical wind observations with two Fabry-Perot interferometers at Poker Flat, Alaska, *J. Geophys. Res.*, **106**, 10,537–10,551, 2001.

Ishii, M., M. Kubota, M. Conde, R. W. Smith, and M. Krynicki, Vertical wind distributions in the polar thermosphere during Horizontal E Region Experiment (HEX) campaign, *J. Geophys. Res.*, **109**, A12311, doi:10.1029/2004JA010657, 2004.

Iwagami, N., S. Komada, and T. Takahashi, Preliminary results of rocket attitude and auroral green line emission rate in the DELTA campaign, *Earth Planets Space*, **58**, this issue, 1107–1111, 2006

Johnson, F. S., W. B. Hanson, R. R. Hodges, W. R. Coley, G. R. Carignan, and N. W. Spencer, Gravity waves near 300 km over the polar caps, *J. Geophys. Res.*, **100**, 23,993–24,002, 1995.

Kosch, M. J., M. Ishii, A. Kohsiek, D. Rees, K. Schlegel, T. Hagfors, and K. Cierpka, Comparison of vertical thermospheric winds from Fabry-Perot interferometer measurements over a 50 km baseline, *Adv. Space Res.*, **26**, 985–988, 2000.

Kurihara, J., T. Abe, K. I. Oyama, E. Griffin, M. Kosch, A. Aruliah, K. Kauristie, Y. Ogawa, S. Komada, and N. Iwagami, Observations of the lower thermospheric neutral temperature and density in the DELTA campaign, *Earth Planets Space*, **58**, this issue, 1123–1130, 2006.

Larsen, M. F. and R. L. Walterscheid., Modified geostrophy in the thermosphere, *J. Geophys. Res.*, **100**, 17,321–17,329, 1995.

Larsen, M. F., A. B. Christensen, and C. D. Odom, Observations of unstable atmospheric shear layers in the lower E region in the post-midnight auroral oval, *Geophys. Res. Lett.*, **24**, 1915–1918, 1997.

Nozawa, S., Y. Ogawa, A. Brekke, T. Tsuda, C. M. Hall, H. Miyaoka, J. Kurihara, T. Abe, and R. Fujii, EISCAT observational results during the DELTA campaign, *Earth Planets Space*, **58**, this issue, 1183–1191, 2006.

Ogasawara, K., K. Asamura, T. Takashima, Y. Saito, and T. Mukai, Rocket observation of energetic electrons in the low-altitude auroral ionosphere during the DELTA campaign, *Earth Planets Space*, **58**, this issue, 1155–1163, 2006.

Parish, H. F., R. L. Walterscheid, P. W. Jones, and L. R. Lyons, Simulations of the thermospheric response to the diffuse aurora using a three-dimensional high-resolution model, *J. Geophys. Res.*, **108**(A4), 1140, doi:10.1029/2002JA009610, 2003.

Price, G. D. and F. Jacka, The influence of geomagnetic activity on the upper mesosphere/lower thermosphere in the auroral zone, I, Vertical winds, *J. Atmos. Terr. Phys.*, **53**, 909–922, 1991.

Price, G. D., R. W. Smith, and G. Hernandes, Simultaneous measurements of large vertical winds in the upper and lower thermosphere, *J. Atmos. Terr. Phys.*, **57**, 631–643, 1995.

Rees, D., R. W. Smith, P. J. Charleton, F. G. McCormac, N. Lloyd, and A. Steen, The generation of vertical winds and gravity waves at auroral latitudes, I, Observations of vertical winds, *Planet. Space Sci.*, **38**, 667–684, 1984.

Rees, M. H., *Physics and Chemistry of the Upper Atmosphere*, Cambridge Atmos. Space Sci. Ser., 298 pp., Cambridge Univ. Press, New York, 1989.

Richmond, A. D. and J. P. Thayer, Ionospheric electrodynamics: a tutorial, in *Magnetospheric Current Systems*, Geophys. Monogr. Ser., vol. 87, edited by S. Ohtani, R. Fujii, M. Hesse, and R. L. Lysac, pp. 131–146, AGU, Washington, D. C., 2000.

Roble, R. G., Energetics of the mesosphere and thermosphere, in *The Upper Mesosphere and Lower Thermosphere: A review of Experiment and Theory*, Geophys. Monogr. Ser., vol. 87, Edited by R. M. Johnson and T. L. Killeen, pp. 1–21, AGU, Washington, D. C., 1995.

Schunk, R. W. and A. F. Nagy, *Ionospheres—Physics, Plasma Physics, and Chemistry*, Cambridge Atmos. Space Sci. Ser., 554 pp., Cambridge Univ. Press, New York, 2000.

Shinagawa, H., S. Oyama, S. Nozawa, S. C. Buchert, R. Fujii, and M. Ishii, Thermospheric and ionospheric dynamics in the auroral region, *Adv. Space Res.*, **31**, 951–956, 2003.

Smith, R. W. and G. Hernandes, Vertical winds in the thermosphere with in the polar cap, *J. Atmos. Terr. Phys.*, **57**, 611–620, 1995.

Sun, Zi-Ping, R. P., Turco, R. L. Walterscheid, S. V. Venkateswaran, and P. W. Jones, Thermospheric response to morningside diffuse aurora: High-resolution three-dimensional simulations, *J. Geophys. Res.*, **100**, 23,779–23,793, 1995.

Thayer, J. P. and J. Semeter, The convergence of magnetospheric energy flux in the polar atmosphere, *J. Atmos. Sol.-Terr. Phys.*, **66**, 807–824, 2004.

Wakabayashi, M. and T. Ono, Electron density measurement under the influence of auroral precipitation and electron beam injection during the DELTA campaign, *Earth Planets Space*, **58**, this issue, 1147–1154, 2006.

Walterscheid, R. L. and L. R. Lyons, The neutral circulation in the vicinity of a stable auroral arc, *J. Geophys. Res.*, **97**, 19,489–19,499, 1992.

Walterscheid, R. L., L. R. Lyons, and K. E. Taylor, The perturbed neutral circulation in the vicinity of a symmetric stable auroral arc, *J. Geophys. Res.*, **90**, 12,235–12,248, 1985.

Williams, B. P., D. C. Fritts, J. D. Vance, C.-Y. She, T. Abe, and E. Thrane, Sodium lidar measurements of waves and instabilities near the mesopause during the DELTA rocket campaign, *Earth Planets Space*, **58**, this issue, 1131–1137, 2006.

T. Abe (e-mail: abe@isas.jaxa.jp), J. Kurihara, N. Iwagami, S. Nozawa, Y. Ogawa, R. Fujii, H. Hayakawa, and K. Oyama